



Response of soil organic carbon to land-use change after farmland abandonment in the karst desertification control

Yating Mu · Runcheng Ye · Kangning Xiong ·
Yue Li · Ziqi Liu · Yidong Long · Lulu Cai ·
Qingping Zhou

Received: 7 December 2023 / Accepted: 1 February 2024 / Published online: 13 February 2024
© The Author(s), under exclusive licence to Springer Nature Switzerland AG 2024

Abstract

Background Land-use change caused by vegetation restoration in karst areas plays an active role in soil carbon sink. However, the response of soil organic carbon (SOC) accumulation and turnover to land-use change after farmland abandonment is still poorly understood.

Methods and aims In this study, we investigated the impacts of converting farmland (maize) (FL) to economic forests [*Juglans regia* L. (walnut) plantation (JP), and *Rosa roxburghii* Tratt plantation (RP)], artificial grassland (AG), or natural grassland (NG) on the distribution of SOC and $\delta^{13}\text{C}$ in the karst desertification control.

Results The SOC stock in the 0–40 cm profile was 67%, 59%, 14%, and 8% higher in RP, JP, AG, and NG than in FL (control). The $\delta^{13}\text{C}$ values in AG, RP, and JP were significantly lower than those in NG and FL at the 0–5 cm depth. It was observed that the $\delta^{13}\text{C}$ increased with soil depth. However, the SOC content decreased. The β values ranged from -6.94 to -3.88 and increased in the order of $\text{RP} < \text{AG} < \text{FL} < \text{JP} < \text{NG}$. Redundancy analysis (RDA) showed that total nitrogen content and soil C/N ratio accounted for significant differences in soil $\delta^{13}\text{C}$ and SOC levels.

Conclusions Our results suggested that economic forests triggered higher SOC accumulation than artificial grassland and natural revegetation after farmland abandonment, but the rate of soil C turnover following afforestation was still higher than that followed by natural revegetation in the short term.

Yating Mu and Runcheng Ye contributed equally to this work and should be considered co-first authors.

Responsible Editor: Tida Ge.

Y. Mu · K. Xiong · Z. Liu · L. Cai
School of Karst Science, Guizhou Engineering Laboratory
for Karst Desertification Control and Eco-industry,
Guizhou Normal University, Guiyang 550001, China

R. Ye · Y. Li (✉) · Y. Long · Q. Zhou
Guiyang Engineering Corporation Limited, Power China,
Guiyang 550081, China
e-mail: liyue_gyy@powerchina.cn

K. Xiong (✉)
State Engineering Technology Institute for Karst
Desertification Control, Guiyang 550001, China
e-mail: xiongkn@163.com

Keywords Soil organic carbon · ^{13}C · Farmland abandonment · Afforestation · Karst desertification

Introduction

Soil organic carbon (SOC) pool is the largest carbon pool in terrestrial ecosystems, and even small changes in it can have significant impacts on the global climate change and the carbon cycle (Battle-Bayer et al. 2010). Land use and management strategies have an impact on SOC stock, and SOC turnover responds

rapidly to climate and land-use changes (Keiblinger et al. 2023; Köchy et al. 2015; Lozano-García et al. 2017, 2020). In the last thousand years, and particularly in the last 200 years, the global population has experienced significant growth, leading to an increased demand for food. By converting natural land into agricultural land, human activities have expedited the mineralization of soil organic matter (SOM) and soil erosion, leading to a carbon loss of approximately 133 Pg in the top 2 m of soil worldwide (Sanderman et al. 2017). Lozano-García et al. (2017) emphasized that the conversion of natural vegetation to agricultural land will result in a significant long-term decrease in SOC stocks. On the contrary, converting farmland to grasslands, shrublands, and forests is considered an effective measure for increasing carbon inputs from vegetation and enhancing SOC sequestration (Han et al. 2023; Li et al. 2012; Veloso et al. 2018). However, there is still some uncertainty regarding the response of SOC turnover to vegetation restoration. Revegetation of sloping farmland or abandoned land may result in land-use changes that can have negative impacts on soil ecological processes and ecosystem functioning (Hu et al. 2010). The rate of soil carbon (C) accumulation after conversion is influenced by factors such as previous land use types, climatic characteristics, soil properties, tree species, and the duration of conversion (Deng and Shangguan 2017; Li et al. 2012; Wang et al. 2018). These factors may complicate the effects of vegetation restoration on SOC turnover. Land-use change affects the carbon sequestration process with varying patterns (Lan et al. 2021; You et al. 2021). Thus, studying the effects of land-use change caused by vegetation restoration on SOC accumulation is crucial for improving soil carbon sink capacity and land management practices.

With the advancement of stable isotope tracer technology, there is a growing utilization of stable carbon isotopes to measure SOC turnover rates, track the source and destination of SOC (degradation, migration, and transformation), and document changes in C3 and C4 vegetation, which can provide valuable insights into environmental changes (Andriollo et al. 2017; Li and Schaeffer 2020; Schellekens et al. 2023). The $\delta^{13}\text{C}$ values in plant C vary with different vegetation types and environmental conditions (Paul et al. 2020). This is due to the unique isotopic fractionation of different SOC during the C cycle under different

plant types, resulting in distinctive $\delta^{13}\text{C}$ values (Liu et al. 2020a). These differences can be reflected by changes in the $^{13}\text{C}/^{12}\text{C}$ ratio of SOC as plant material enters the soil system (Qiao et al. 2015). Han et al. (2015) showed that plant functional types are important in controlling SOC content and vertical variation of $\delta^{13}\text{C}_{\text{SOC}}$. Paul et al. (2020) reported that the average increase in SOM $\delta^{13}\text{C}$ values with depth is primarily attributed to changes in vegetation $\delta^{13}\text{C}$ values over the past 20,000 years. In addition, the composition of soil $\delta^{13}\text{C}$ is also influenced by climate, soil type, soil properties, and other factors (Wang et al. 2017; You et al. 2021). The vertical enrichment of the soil $\delta^{13}\text{C}$ has been shown to correlate with SOC turnover, and the slope of the linear regression (β) of the logarithm of the SOC concentration in the soil profile on the $\delta^{13}\text{C}$ value could reflect the dynamics of SOC, the lower the β value, the faster the SOC decomposition rate (Acton et al. 2013; Garten et al. 2000; Wang et al. 2017). Understanding the variation of the $\delta^{13}\text{C}_{\text{SOC}}$ value along soil profiles helps to explain the accumulation or consumption of SOC after land use conversion. This method has been widely used to assess soil C turnover dynamics on a global scale (Wang et al. 2018). But most of these studies focus on alpine ecosystems (Huang et al. 2022; Li et al. 2020; Zhao et al. 2019) and temperate ecosystems in northern China (Che et al. 2022; Qu et al. 2022; You et al. 2021). However, few studies have focused on subtropical karst ecosystems (Han et al. 2020). Therefore, it is necessary to study the impacts of land-use changes on the vertical distribution of $\delta^{13}\text{C}$ to accurately assess the benefits of ecological restoration in the karst region.

Karst landscapes are widespread throughout the world, and surface and near-surface karst outcrops cover 20% of the planet's ice-free arid areas (Ford and Williams 2007). As the world's largest karst ecosystem, the karst region of southwestern China is experiencing serious soil erosion, regional rock desertification, and the progressive impoverishment of local residents because of its unique geological background, extensive karstification, and unsustainable land use in the modern era (Chen et al. 2021; Dai et al. 2018). Against the seriousness of this issue, the Chinese government launched the "Green for Grain" program in 1999. This program aims to convert slope farmland to forests or grasslands, thereby reducing soil erosion and restoring the region's damaged

ecosystem. The treatment of karst rocky desertification is typically characterized by farmland abandonment, which serves as a prime example of vegetation restoration in ecologically fragile areas worldwide (Xiao and Xiong 2022). This approach has led to a substantial enhancement of regional ecosystem services (Cai et al. 2023). The SOC storage capacity is affected by the evolution of rocky desertification (Wang et al. 2022a). And changes in land use have a significant impact on SOC accumulation. However, there is still a lack of understanding of the mechanism of soil C turnover after farmland abandonment in the karst desertification control. Ahmed et al. (2012) reported that karst soils are rich in organic matter, with more than 66% of SOC stored in the upper 0–30 cm soil layer. The SOC pool in karst regions is more susceptible to environmental factors due to the relatively high level of microbial activity in the upper soil layers. In recent years, many researchers have come to agree that the karstification and land use changes in southwest China may be able to act as a carbon sink in the global carbon cycle (Tong et al. 2018; Zeng et al. 2016). This helps to explain the natural phenomenon of the “C missing sink” in the global C balance. The history of aboveground vegetation affects soil quality restoration in degraded ecosystems and inevitably influences SOM dynamics during the restoration process. Land-use change is an important factor that directly affects carbon storage patterns in karst areas (Li et al. 2022; Wang et al. 2022b; Zhang et al. 2020). $\delta^{13}\text{C}$ analysis is an effective tool to examine the degree of soil quality recovery during the restoration process of degraded ecosystems (Chen et al. 2002). Therefore, studying the response of SOC and soil $\delta^{13}\text{C}$ to land-use change after farmland abandonment in the karst desertification control is of great importance to understand the mechanisms by which land-use change affects SOC in karst ecosystems.

Therefore, in order to clarify the relationship between land-use change after farmland abandonment and the accumulation of SOC and the turnover of soil C in the karst desertification control. Here, we estimated the SOC stocks in the soil profiles of *J. regia* plantation (JP), *R. roxburghii* plantation (RP), artificial grassland (AG), natural grassland (NG), and farmland (FL) (control). We also analyzed the trend of $\delta^{13}\text{C}$ values with depth, and compared the SOC turnover rates under different land uses using soil

profile organic carbon content and corresponding $\delta^{13}\text{C}$ values. The objectives of this study were (1) to elucidate the effects of land-use change after farmland abandonment on the distribution of SOC and soil $\delta^{13}\text{C}$ and the main controlling factors; (2) to compare the differences in SOC turnover rates among the five land uses. We hypothesized that (1) the $\delta^{13}\text{C}_{\text{SOC}}$ values in the topsoil layer under all land uses were significantly different due to the differences in C input sources from vegetation; (2) All of the converted land uses had increased SOC stocks and accelerated SOC turnover rate compared with farmland. This study is instructive for soil carbon management in ecologically fragile karst ecosystems.

Materials and methods

Study site

The study site is located at the Salaxi Field Observation Station of the State Research Center for Karst Desertification Prevention Engineering Technology in Bijie City, Guizhou Province, Southwest China (105°01'12"~105°08'38" E, 27°11'09"~27°17'28" N) (Fig. 1). The study area is dominated by a plateau mountain terrain with significant relief, 1500–2180 m above sea level. The average annual temperature of this region is 12.8 °C, and the annual rainfall is about 984.4 mm, belonging to north subtropical humid monsoon climate. The rainy season, which accounts for 52% of the annual rainfall, lasts from June to September. The lithology in this area is mainly limestone. The main soil type is zonal yellow soil, with lime soil and yellow brown soil being distributed in a smaller range.

Zea mays L. (Maize) has been a staple crop in the region, but long-term extensive management has resulted in vegetation destruction, severe soil erosion, the exposure of large rocks, and significant rock desertification. These issues have further exacerbated local poverty. Since 2010, large-scale ecological restoration projects have been implemented by the Chinese government in this area to promote rocky desertification control. Most of the cultivated lands were abandoned, allowing the recovery of vegetation (through natural revegetation, grass planting, and afforestation programmes). *Juglans regia* L. belongs to the family Juglandaceae and exhibits strong

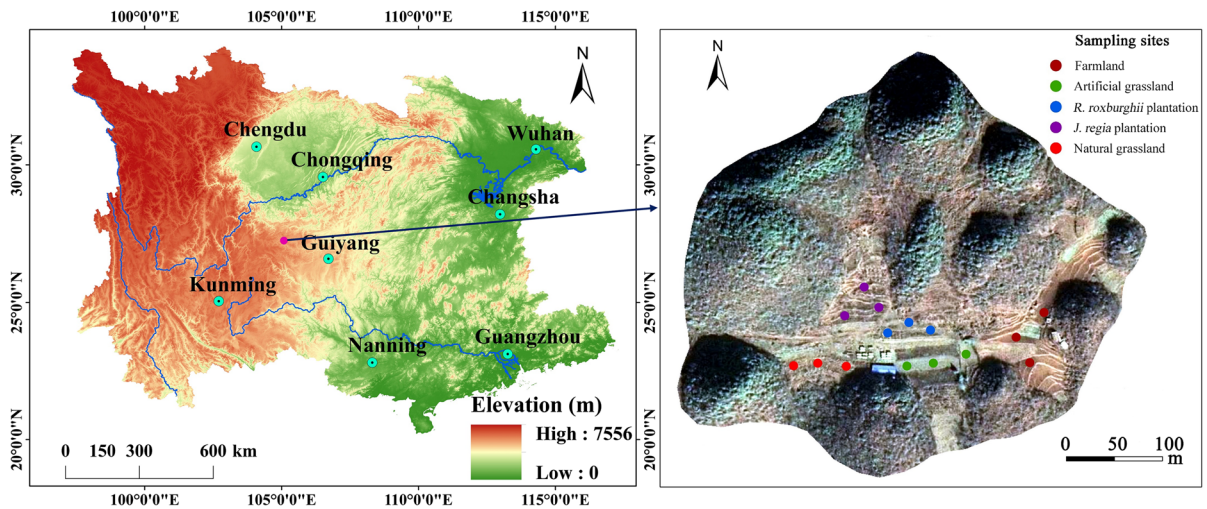


Fig. 1 Location of study area and sampling sites

drought tolerance. It can grow rapidly in karst areas with calcareous soil and harsh habitat conditions, making it effective in reversing desertification (Chen et al. 2009). *Rosa roxburghii* Tratt, belonging to the Rosaceae family, possesses the traits of rapid growth and robust adaptability. It can thrive in arid and infertile soil conditions commonly found in karst areas. *J. regia* and *R. roxburghii* have been widely used as pioneer species in forest ecological restoration in this region, due to their significant economic and ecological value. Artificial grass planting was used to increase vegetation cover and prevent soil erosion in the karst desertification control. *Lolium perenne* (L.) is the dominant plant species in artificial grasslands. At the same time, due to the export of rural labor force caused by “rocky desertified cropland” under karst geological background, the abandonment of farmland occurred frequently and allowed the natural recovery of grasslands in this region, and the dominant species were *Neyraudia reynaudiana* (K.) Keng, *Miscanthus floridulus* (L.) Warb, and *Imperata cylindrical* (L.) Beauv. Additionally, a portion of the land has been maintained as farmland using traditional practices. These sites had been cultivated for at least 100 years before the conduct of vegetation restoration. For the present study, we selected the farmland (specifically a maize field) as the control to investigate the effects of land-use changes after farmland abandonment on SOC stocks and $\delta^{13}\text{C}$ values in soil profiles. All five land uses selected for this study were

adjacent to each other and had the same geochemical background and soil type. More details can be found in Table 1.

Soil sampling and analyses

In August 2020, 10 years after restoration commenced, the collection of soil samples in the field was completed. Three sampling plots were set up under the same land use (JP, RP, AG, NG, and FL), and three sampling points were selected for each plot. Five soil cores were randomly collected from each sampling point at five depths (0–5 cm, 5–10 cm, 10–20 cm, 20–30 cm, and 30–40 cm) using a 5-cm diameter soil auger connected to a handle with marking scales. Soil samples from three sampling points in the same plot were mixed according to depth. They were then divided into two parts: one part was placed in an aluminum box and dried at 105 °C for 24 h for the determination of the gravimetric soil water content (SWC, %), and the other part was taken back to the lab in a self-sealing bag to air dry. At the same time, a stainless-steel cutting ring with a volume of 100 cm³ was used to collect undisturbed soil cores at the same depth in the vicinity of the drilled soil cores. The soil cores were then dried at 105 °C until a constant weight was achieved in order to determine the soil bulk density (BD). Natural air-drying of soil samples was conducted, followed by the removal of roots and plant material. The samples were then ground into a fine powder and passed through a 100-mesh sieve

Table 1 Description of the study site

	Land use	Slope (°)	Elevation (m)	Vegetation coverage (%)	Management measures
	JP	15	1900	70–82	Artificial management.
	RP	10	1895	75–89	Artificial management.
	NG	9	1892	75–90	No human activities.
	AG	9	1892	80–92	Ploughed and fertilized in the planting year; harvested 3–4 times per year.
<i>JP</i> , <i>J. regia</i> plantation; <i>RP</i> , <i>R. roxburghii</i> plantation; <i>NG</i> , natural grassland; <i>AG</i> , artificial grassland; <i>FL</i> , farmland	FL	8	1893	60–73	Ploughed 1–2 times per year; fertilized with inorganic fertilizers and farm manure.

(0.15 mm diameter). Air-dried sifted soil samples were treated with 0.5 mol/L HCl at 25 °C for 24 h to remove carbonates (Midwood and Boutton 1998). Afterward, they were washed with distilled water until neutral and dried at 60 °C. The samples were then crushed and stored for analysis. The total nitrogen (TN) and SOC contents were measured using an elemental analyzer (FlashSmart, Thermo Fisher Scientific Inc., Waltham, MA, USA). The soil $\delta^{13}\text{C}$ was measured using the EA-IRMS system (EA Isolink & Delta V Advantage, Thermo Fisher Scientific Inc., Waltham, MA, USA).

$\delta^{13}\text{C}$ value represents the relative difference between the ratio of two carbon isotopes in a sample and a corresponding ratio in a standard sample. It is an indicator used to describe the degree of variation in the natural abundance of $\delta^{13}\text{C}$ when comparing a sample with a standard sample (Breecker et al. 2015). The calculation formula is as follows:

$$\delta^{13}\text{C} = (R_{\text{sample}}/R_{\text{standard}} - 1) \times 1000\text{‰} \quad (1)$$

where R_{sample} is the $^{13}\text{C}/^{12}\text{C}$ ratio of the sample and R_{standard} is the $^{13}\text{C}/^{12}\text{C}$ ratio of the Vienna Pee Dee Belemnite (VPDB) standard. The analytical precision of $\delta^{13}\text{C}$ was $\leq 0.1\text{‰}$.

Calculations

The SOC stocks (Mg ha^{-1}) at different soil depths were calculated as follows (Li et al. 2021):

$$\text{SOC}_{\text{stock}} = \text{SOC} \times \text{BD} \times D \times 10^{-1} \quad (2)$$

Where *SOC* is the measured SOC content (g kg^{-1}); *BD* is the soil bulk density (g cm^{-3}); *D* represents the

thickness of the soil depth (cm). The SOC stock in the entire 0–40 cm profile was the sum of each soil layer.

Statistical analysis

The slope of a linear regression (β) relating soil $\delta^{13}\text{C}$ value to the log-transformed SOC content was used to describe the SOC turnover rate under different land-use types. All data were checked for the homogeneity of variances and normality before applying ANOVA. Two-way ANOVA was performed to detect the effects of land uses, soil depths and their interaction (land-use * depths) on SOC contents, SOC stocks, $\delta^{13}\text{C}$ values, and soil physicochemical properties. One-way ANOVA was conducted to evaluate significant differences with respect to different land uses. *Turkey* HSD post hoc tests were further conducted to assess differences among means at the level of $p < 0.05$. The IBM SPSS Statistics 24 (IBM Inc., Armonk, NY, USA) was used to conduct statistical analyses. Relationships of SOC and $\delta^{13}\text{C}$ between soil physicochemical properties were analyzed using a linear regression model with Origin 2021 software (Origin Software Inc., Fairview, TX, USA). Redundancy analysis (RDA) from the CANOCO 5.0 software (Microcomputer Power, Ithaca, NY, USA) was used to determine the proportions of variability in $\delta^{13}\text{C}$ and the content of SOC explained by soil physicochemical variables. Automatic forward selection of variables sorted the importance of each explanatory factor. The significance of the RDA was assessed using a Monte Carlo permutation with 499 iterations.

Results

Changes in SOC stock

The two-way ANOVA results indicate that land-use types, soil depths, and their interaction significantly ($p < 0.05$) influenced the level of SOC stock (Table 2). In order to test our second hypothesis, FL was used as the contrast to evaluate the effects of land-use changes after farmland abandonment on SOC stocks. At the 0–5 cm depth, the mean SOC stock in RP was significantly higher than that in other land uses ($P < 0.05$) (Fig. 2A). And the SOC stocks in RP and JP were both significantly higher than that in FL at the depth of 5–40 cm. The SOC stock reached its maximum value at the depth of 10–20 cm along the soil profile under different land uses. In the whole

0–40 cm soil profile, the SOC stocks in RP, JP, AG, NG, and FL were 83.9, 80.3, 57.3, 54.7, and 50.4 Mg ha⁻¹, respectively. Compared with FL, land conversion increased SOC stocks (Fig. 2B). The SOC stock at depths of 0–40 cm was 67%, 59%, 14%, and 8% higher in RP, JP, AG, and NG, respectively, than in FL.

$\delta^{13}\text{C}$, SOC content, and β values

In line to our first hypothesis, we found that land-use type and soil depth and their interactions significantly affected the $\delta^{13}\text{C}$ and SOC content (Table 2, $P < 0.01$). In general, the $\delta^{13}\text{C}$ values in SOC showed a similar vertical variation trend along soil profiles under different land uses (Fig. 3A). With the increase of soil depth, the $\delta^{13}\text{C}$ value gradually increased. The

Table 2 Two-way analysis of variance of the effect of land-use and soil depth on soil variables

Soil variables	Land-use			Depth			Land-use * Depth		
	df	F	P-value	df	F	P-value	df	F	P-value
SOC content	4	32	<0.001	4	77	<0.001	16	3	0.004
$\delta^{13}\text{C}$	4	27	<0.001	4	117	<0.001	16	5	<0.001
SOC stock	4	24	<0.001	4	19	<0.001	16	3	0.013
SWC	4	32	<0.001	4	21	<0.001	16	2	0.121
BD	4	10	<0.001	4	71	<0.001	16	4	<0.001
TN	4	16	<0.001	4	235	<0.001	16	8	<0.001
C/N	4	190	<0.001	4	11	<0.001	16	7	<0.001

SOC, soil organic carbon; SWC, soil water content; BD, bulk density; TN, total nitrogen; C/N, C/N ratio. *df* represents the degree of freedom, *F* represents the ratio of two mean squares

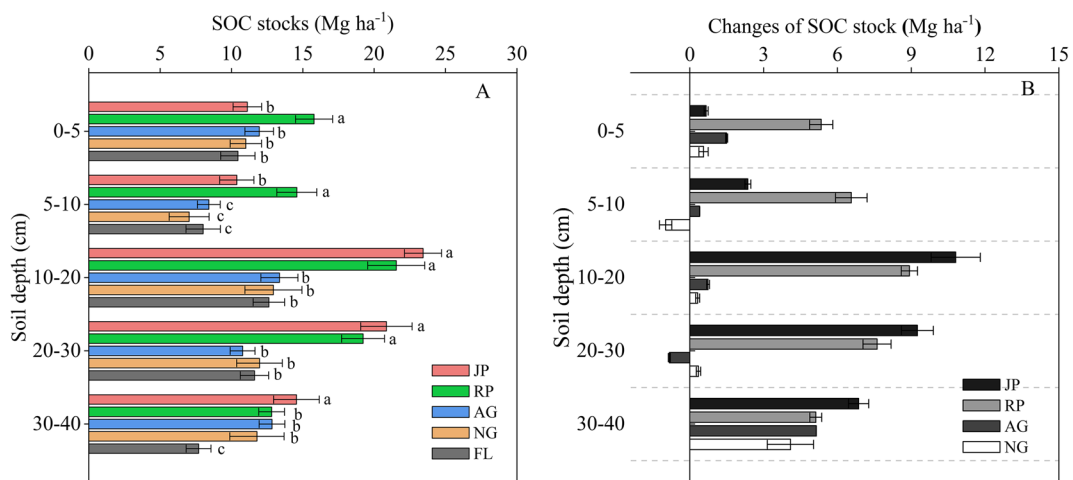


Fig. 2 Vertical distribution of SOC stock (A) and vertical changes in SOC stock (B) relative to farmland along the profiles. JP: *J. regia* plantation; RP: *R. roxburghii* plantation; AG: artificial grassland; NG: natural grassland; FL: farmland. Values are means ($n=3$) with standard error. Significant differences were indicating with different lowercase letters ($p < 0.05$)

artificial grassland; NG: natural grassland; FL: farmland. Values are means ($n=3$) with standard error. Significant differences were indicating with different lowercase letters ($p < 0.05$)

$\delta^{13}\text{C}$ values of the subsurface soil layer were 1.10‰ to 3.40‰ higher than those of the 0–5 cm soil layer in all land uses. The mean $\delta^{13}\text{C}$ values in FL (-23.50‰) and NG (-23.66‰) were significantly higher than that in AG (-24.54‰), JP (-24.63‰), and RP (-25.00‰) at the depth of 0–5 cm ($P < 0.05$) (Fig. 3A). But below the 0–5 cm depth, no significant difference was detected between FL and the converted land uses except JP.

The content of SOC in mineral soil profiles showed a decreasing trend from surface to subsoil layer in all land uses (Fig. 3B). The SOC content in RP and JP was significantly higher than that in NG, FL, and AG at the depth of 0–30 cm ($P < 0.05$). However, no significant differences were found for SOC content under different land uses at the depth of 30–40 cm (Fig. 3B).

In the present study, the regression slope (β) of the linear relationship between $\delta^{13}\text{C}$ value and the log-transformed SOC content was used as a proxy of SOC turnover (Fig. 4). The linear regression fit well for all five land uses, judging by the R^2 and p values. Specifically, the β values ranged from -6.94 to -3.88 (Fig. 4), which increasing in the order of $\text{RP} < \text{AG} < \text{FL} < \text{JP} < \text{NG}$. The highest β value was observed in NG, and lowest in RP.

SWC, BD, TN, and C/N ratio

Soil physicochemical properties differed significantly among land uses and depths (Table 2, $P < 0.001$). Meanwhile, the BD, TN, and C/N ratio were all

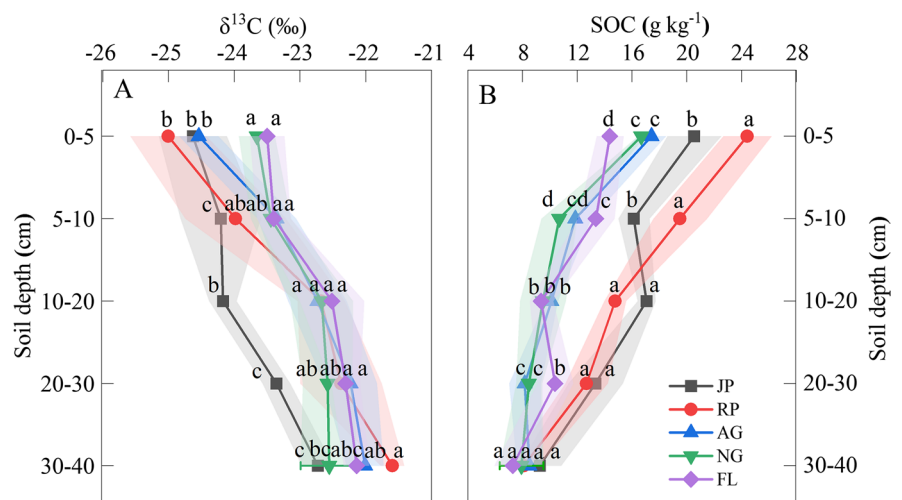
significantly affected by the interactions of land-use types and soil depths (Table 2). However, the SWC was not significantly affected by the interactions ($P > 0.05$; Table 2).

Specifically, the SWC in NG and AG was higher than that in RP, JP, and FL in the entire 0–40 cm soil profile (Fig. 5A). The BD was highest in RP at the depth of 5–10 cm. And the BD in JP and RP was higher than that in NG, AG, and FL at the depth of 20–40 cm (Fig. 5B). At the 0–10 cm depth, the TN contents were similar in NG and FL but higher than AG, RP, and JP. AG and NG had similar TN contents which were higher than that in RP and FL at the depth of 10–40 cm (Fig. 5C). RP and JP had higher C/N ratios as compared to AG, FL, and NG at 0–40 cm soil depths (Fig. 5D). Generally, the profile patterns of SWC and soil TN content showed a decreasing trend, while the soil BD increased along soil profiles in all land uses.

Factors affecting soil $\delta^{13}\text{C}$ and SOC

The relationships between soil $\delta^{13}\text{C}$ and soil physicochemical properties were tested using linear regression analysis. Results of regression analyses showed that the $\delta^{13}\text{C}$ values in different soil depths were positively correlated with BD (Fig. 6A), while they were negatively related to SWC and TN (Fig. 6B, C). The $\delta^{13}\text{C}$ value was positively correlated with C/N in FL, while an inverse relationship was detected between the $\delta^{13}\text{C}$ and C/N in AG (Fig. 6D).

Fig. 3 Vertical distribution of $\delta^{13}\text{C}$ values (A) and SOC content (B) under different land uses. JP: *J. regia* plantation; RP: *R. roxburghii* plantation; AG: artificial grassland; NG: natural grassland; FL: farmland. Values are means ($n = 3$) with standard error. Significant differences were indicating with different lowercase letters ($p < 0.05$)



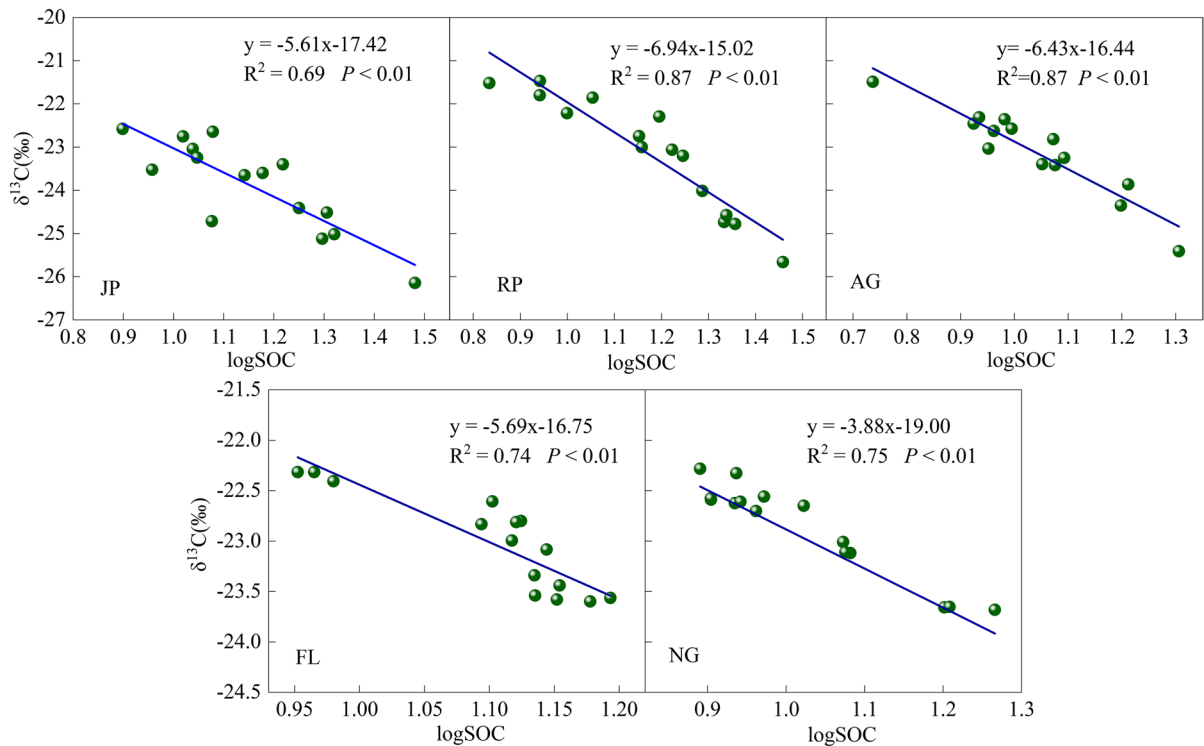


Fig. 4 The linear regression between $\delta^{13}\text{C}$ and log-transformed SOC content under different land uses. The slope of linear regression is defined as β value. JP: *J. regia* plantation;

RP: *R. roxburghii* plantation; AG: artificial grassland; NG: natural grassland; FL: farmland

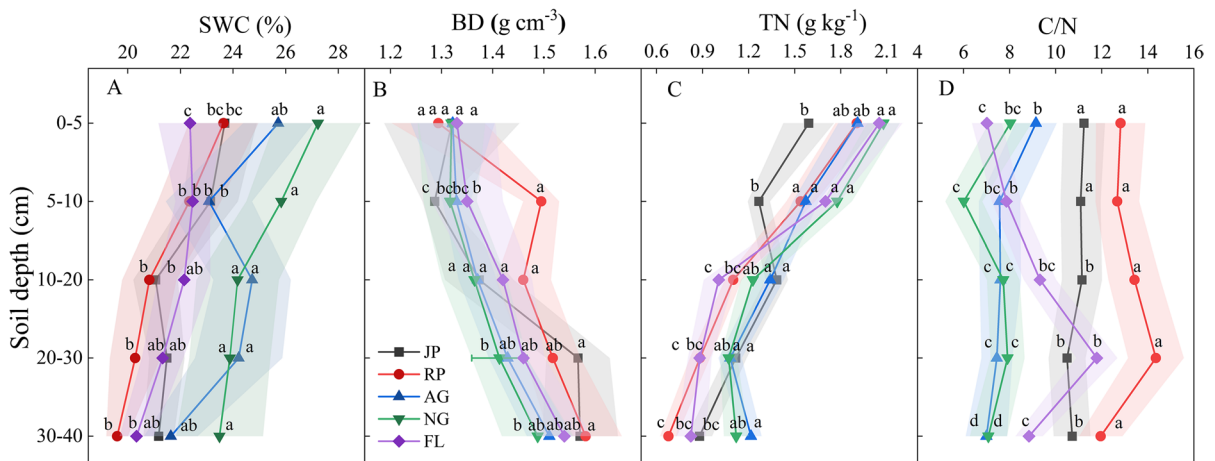


Fig. 5 Vertical distribution of soil physicochemical properties under different land uses. **A** vertical distribution of soil water content (SWC) under different land uses; **B** vertical distribution of soil bulk density (BD) under different land uses; **C** vertical distribution of total nitrogen (TN) under different land

uses; **D** vertical distribution of C/N under different land uses. JP: *J. regia* plantation; RP: *R. roxburghii* plantation; AG: artificial grassland; NG: natural grassland; FL: farmland. Values are means ($n=3$) with standard error. Significant differences were indicating with different lowercase letters ($p < 0.05$)

Table 3 Results of RDA analysis of soil $\delta^{13}\text{C}$ and SOC content in relation to edaphic factors determined by interactive forward selection procedure with unrestricted permutation tests

Name	Explains (%)	Contribution (%)	pseudo-F	P
TN	50.2	58.7	23.2	0.002
C/N	33.1	38.7	43.8	0.002
BD	2.2	2.5	3.2	0.086
SWC	<0.1	0.1	0.1	0.832

TN, total nitrogen; C/N, C/N ratio; BD bulk density, SWC, soil water content

The effects of soil physicochemical properties on the soil $\delta^{13}\text{C}$ and SOC content were assessed by RDA. The RDA showed that edaphic factors accounted for 85.64% of the total variation in soil $\delta^{13}\text{C}$ and SOC content (Fig. 7). The Monte Carlo permutation test showed that the variations in $\delta^{13}\text{C}$ and SOC content were explained by the first two axes, with the first axis explaining 83.15% and the second axis explaining 2.49% (Fig. 7). A forward selection of the explanatory variables indicated that $\delta^{13}\text{C}$ value and SOC content were mainly influenced by TN and soil C/N ratio (Table 3). TN explained most variations in $\delta^{13}\text{C}$ and SOC content (50.2%), followed by the C/N ratio (33.1%).

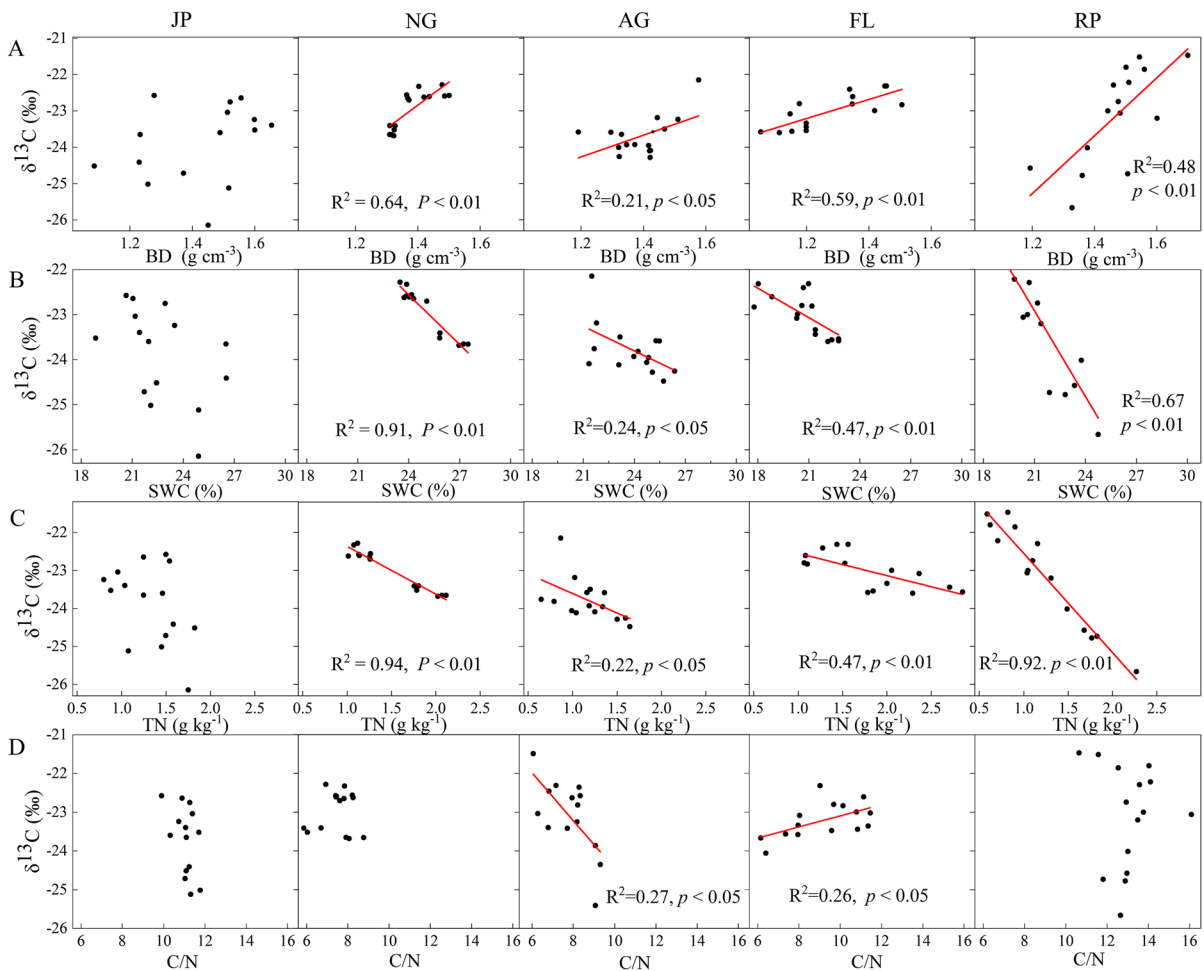


Fig. 6 Relationships between soil $\delta^{13}\text{C}$ and edaphic factors. **A** relationship between soil $\delta^{13}\text{C}$ and soil bulk density (BD); **B** relationship between soil $\delta^{13}\text{C}$ and soil water content (SWC); **C** relationship between soil $\delta^{13}\text{C}$ and total nitrogen (TN);

D relationship between soil $\delta^{13}\text{C}$ and C/N. JP: *J. regia* plantation; RP: *R. roxburghii* plantation; AG: artificial grassland; NG: natural grassland; FL: farmland

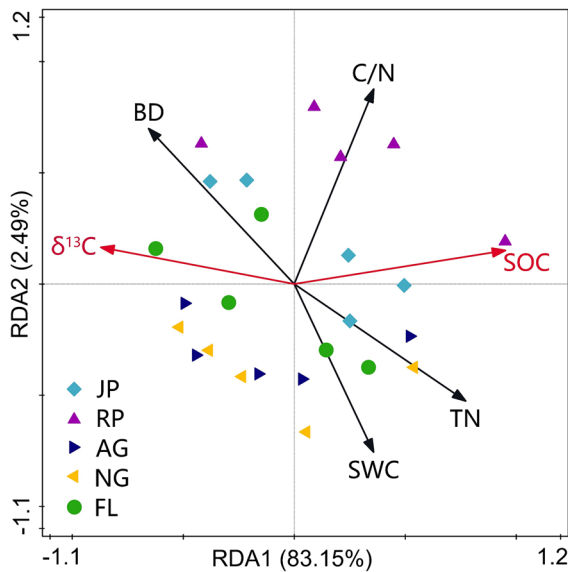


Fig. 7 Redundancy analysis (RDA) ordination diagram for soil $\delta^{13}\text{C}$ and SOC content with edaphic factors under different land uses. SOC: soil organic carbon; TN: total nitrogen; C/N: C/N ratio; BD: bulk density; SWC: soil water content. JP: *J. regia* plantation; RP: *R. roxburghii* plantation; AG: artificial grassland; NG: natural grassland; FL: farmland

Discussion

Impacts of land-use change on SOC stock

Previous studies have demonstrated that farmland abandonment in karst areas promotes the recovery and storage of SOC (Liu et al. 2020b). In the present study, after 10 years of land conversion, the SOC stocks in the 0–40 cm soil profiles increased by 8–67% under different land uses. The RP had 67% higher SOC stock compared with the farmland at 0–40 cm depths (Fig. 2B). The soil microbial community in karst soils contributes substantially to the enhancement of SOC stocks after agricultural abandonment in degraded karst landscapes (Guo et al. 2021). The surface of RP contains a significant amount of fresh litter and abundant microorganisms, which enhances the input of SOM into the soil (Jobbágy and Jackson 2000). And a higher vegetation cover in the RP can also reduce surface runoff and sediment redistribution, thereby reducing soil erosion and the associated loss of SOC (Dong et al. 2022). About 59% higher SOC stock was found in JP compared with the farmland at 0–40 cm soil depths (Fig. 2B). Zhang

et al. (2017) found that the planting of *J. regia* has the potential to not only restore vegetation but also sequester high amounts of carbon in the karst region of Southwest China. Previous studies have reported that the concentration of SOC in plantation forests are often influenced by soil conditions, wood type, and tree components (Cheng et al. 2015; Di and Huang 2022; Zhao et al. 2023). The surface litter of JP was sparse and difficult to decompose, leading to a slow decomposition process and resulting in low storage of SOC in the surface layer (0–10 cm). Soil bulk density in the soil layer below 10 cm significantly increased in JP (Fig. 5B), porosity decreased and microbial activity weakened, which inhibited the decomposition of SOM to a certain extent and promoted the accumulation of SOC. Additionally, fine root production enhances the SOC stock in the subsurface soil layers (Kengdo et al. 2023). Therefore, the SOC stock in the subsurface layer was significantly higher than that in the surface layer. About 14% higher SOC stock was found in the entire 0–40 cm profile of artificial grasslands compared with farmland (Fig. 2B). However, this was still significantly lower than the SOC stocks in RP and JP. SOC storage in soils is driven by inputs throughout the entire soil profile (Hobley et al. 2017). Herbaceous plants grow slowly in the early stages, the litter and root systems of plants in grasslands are underdeveloped, and early new vegetation is less productive. This leads to a lower input of SOM and a more uniform distribution of SOM (Zhao et al. 2022). Our results also showed that the SOC stock of natural grassland increased by only 8% compared with farmland at the depth of 0–40 cm (Fig. 2B). The possible reason is that vegetation restoration and less soil disturbance after farmland abandonment can improve soil structure to some extent. This condition is conducive to a series of soil microbial activities and the stabilization of SOC (Han et al. 2023). However, the low-grade of secondary vegetation succession, less surface litter and fewer inputs of fresh SOM, and SOC recovery is slow in the short abandoned time (Liu et al. 2020b). As a result, the increase in SOC stock in NG was less than that in RP, JP, and AG.

Changes in $\delta^{13}\text{C}$ with depth after land conversion

Our results showed that the average $\delta^{13}\text{C}$ values at different soil depths in all land uses ranged from -25.00‰ to -21.59‰ . This result agrees with the

study of Zhu and Liu (2006) which found that the $\delta^{13}\text{C}$ value variation of SOC for yellow soil profiles in karst areas ranges from -24.8‰ to -21.1‰ , from surface to bottom of soil profiles. In this study, the $\delta^{13}\text{C}$ values in the 0–5 cm soil layer indicated that FL had significantly higher values compared with other land uses, except for NG. The surface vegetation of RP, JP, and AG consisted of C3 cycle plants, which had been converted from C4 cycle plants (maize) with higher $\delta^{13}\text{C}$ values. Therefore, the $\delta^{13}\text{C}$ value of the soil surface decreased due to the influence of carbon input sources from vegetation. However, no significant difference in $\delta^{13}\text{C}$ was found between FL and NG at the 0–5 cm depth. Below that depth, there were no significant difference in $\delta^{13}\text{C}$ between land uses except JP. This was most likely a result of the masking effect of previous plant residues or soil microorganisms (Boström et al. 2007). That is, the decomposition of newly inputted residues in soil profiles after land-use conversion may be influenced by old residues (from previous land uses) that have not fully decomposed. Therefore, the variation of $\delta^{13}\text{C}$ value was slow at the deeper soil depths, and it may be difficult to detect the effects of land-use changes on $\delta^{13}\text{C}$ below the 0–5 cm depth just over the 10 years experimental period in this study.

The $\delta^{13}\text{C}$ values showed an increasing trend along the soil profiles, which was opposite to that of SOC content (Fig. 3). The results were in agreement with previous relevant studies in karst areas (Han et al. 2015; Lan et al. 2021; Liu et al. 2019). The increase of $\delta^{13}\text{C}$ values along the soil profile is typical of well-drained soil (Bird et al. 2001). The karst area has a thin soil layer, poor soil quality, deep groundwater burial, and a limited capacity to retain soil water and fertilizer. Therefore, the karst mountain area has good drainage conditions, which can significantly promote SOM turnover. The enrichment values of soil $\delta^{13}\text{C}$ along soil profiles in RP, AG, JP, FL, and NG were 3.40‰, 2.54‰, 1.90‰, 1.36‰, and 1.10‰, respectively. However, Han et al. (2020) found that the vertical changes in $\delta^{13}\text{C}$ were 6‰ to 11‰ along soil profiles under land-use changes in karst areas. The magnitude of change in $\delta^{13}\text{C}$ with depth was significantly larger than that observed in our study. Zhu and Liu (2006) found that the vertical patterns of $\delta^{13}\text{C}$ in SOM exhibit distinct regional characteristics in karst areas. The differences in vertical enrichment of $\delta^{13}\text{C}$ can be explained by variations in the quality

and quantity of carbon input from plants, as well as the subsequent carbon cycling processes in soil profiles (Wang et al. 2017). Besides, the shorter land fallow years (10 years) in this study may be a factor leading to the lower $\delta^{13}\text{C}$ gradients within soil profiles. Because the composition of surface SOC is still partly derived from previous C4 plants in addition to fresh carbon assimilates (Krull et al. 2005).

The vertical enrichment of soil $\delta^{13}\text{C}$ can be interpreted by the following processes: (1) The mixing of organic matter inputs with differing isotopic compositions. In this study, vegetation had changed between C3 and C4 plants for RP, JP, and AG, resulting in a change in the isotopic signatures of C inputs. Furthermore, the vertical enrichment of $\delta^{13}\text{C}$ may be closely related to the “Suess Effect”. This effect refers to the depletion of CO_2 isotopes in the atmosphere due to the burning of ^{13}C fossil fuels and biomass (Friedli et al. 1986). As a result, the $\delta^{13}\text{C}$ values of surface SOM correspond to the negative $\delta^{13}\text{C}$ values of litters (Breecker et al. 2015). The deeper the soil layer, the more enriched the old SOC becomes with $\delta^{13}\text{C}$, while the upper soil layer experiences a depletion of $\delta^{13}\text{C}$, resulting in the enrichment of new SOC. Therefore, soil $\delta^{13}\text{C}$ values are enriched along the profile (Boström et al. 2007; Wynn et al. 2006). However, based on an archive of soil samples dating back 100 years and modern samples taken from the same sites in the Russian steppe, Torn et al. (2002) found that the $\delta^{13}\text{C}$ profiles of soils appeared similar in modern and pre-industrial times. This suggests that the accumulation of $\delta^{13}\text{C}$ with soil depth is not caused by the depletion of atmospheric $^{13}\text{CO}_2$ from the combustion of fossil fuels. In addition, many studies have shown that root $\delta^{13}\text{C}$ is usually more enriched than aboveground biomass (especially leaves or branches) from the same plant (Garten et al. 2000; Powers and Schlesinger 2002). Thus, if the C in deep soils is derived primarily from root litter, and the topsoil C is mainly derived from leaf and branch litter, then the soil $\delta^{13}\text{C}$ becomes enriched with depth (Wynn et al. 2006). However, the validity of this hypothesis is questionable when the contribution of root litter to topsoil C is greater than that of aboveground biomass. (2) Kinetic fractionation during the maturation of SOC. The increase of the $\delta^{13}\text{C}$ value with increasing soil depth is related to the isotopic fractionation effect caused by the fact that microorganisms tend to utilize the ^{13}C -depleted carbon sources in the environment

during the degradation of SOM. The accumulation of ^{13}C recombination fraction in the decomposing substrates eventually returns to SOM (Garten et al. 2000; Li and Schaeffer 2020; Powers and Schlesinger 2002; Wynn et al. 2005). That is, the spatial variation of the $\delta^{13}\text{C}$ value with depth in the same soil profile reflects the temporal variation of the $\delta^{13}\text{C}$ value during SOM decomposition. This indicates that the process of SOM decomposition has distinct stages (Chen et al. 2002). When isotope fractionation is the dominant mechanism of the enrichment of $\delta^{13}\text{C}$ along the soil profile, the increase of $\delta^{13}\text{C}$ with depth can effectively indicate the dynamics of soil C turnover (Acton et al. 2013).

Effects of land uses on SOC turnover

Differences in plant biomass under various vegetation covers directly impact the input of organic matter into the soil through plant litter and root exudates (Jobbágy and Jackson 2000). Previous studies have found that the abandonment of agricultural lands can enhance the SOC stock with varying patterns in the karst region (He et al. 2022; Hu et al. 2018; Lan et al. 2021; Xiao et al. 2017). In the present study, we investigated the effects of land-use changes on the distribution of SOC and $\delta^{13}\text{C}$ after farmland abandonment using farmland as a control. The vertical enrichment of soil $\delta^{13}\text{C}$ has been shown to be correlated with the turnover of soil C. The amplitude of the $\delta^{13}\text{C}$ value rise in different soil profiles reflects the intensity of the carbon isotope fractionation effect during the decomposition of SOM. The greater the rise amplitude, the stronger the fractionation effect. This means that the decomposition degree of SOM is higher (Wedin et al. 1995). In the present study, the fractionation effect of SOC isotopes in the RP soil was the strongest, indicating a lower stabilization of SOC. The linear regression slope (β) between the logarithm of SOC content and the $\delta^{13}\text{C}$ value in the soil profile is used to represent the rate of SOC decomposition, a lower β value indicates a higher SOC turnover rate (Acton et al. 2013; Gautam et al. 2017; Garten 2006; Wang et al. 2018). The results showed that the β values ranged from -6.94 to -3.88 across all land uses and increased in the following order: $\text{RP} < \text{AG} < \text{FL} < \text{JP} < \text{NG}$ (Fig. 4). SOC serves as a key factor in driving microbial community composition, and microbial activity has an important effect on the stability and sequestration of

SOC (Chen et al. 2023a, b). The RP with the lowest β value indicated a faster turnover rate of SOC compared with other land uses. This is attributed to the abundance of surface litter and microbial activity in RP. Additionally, there is some degree of mineralization of SOM in RP as a result of frequent exposure to human activities. Therefore, the SOC content in the RP had lower stabilization. Grass-derived C is more easily decomposed by soil microbes, and increased microbial activity further enhances the cycling of SOC (You et al. 2019). The β value of the artificial grassland (-6.43) was slightly higher than that of RP (-6.94) (Fig. 4), indicating that artificial grasslands had the second highest SOC decomposition rate after RP. Organic C fractionation in the surface soil in JP was smaller than that in RP and AG because of the slow decomposition of the surface litter. Therefore, a higher β value was found in JP than in RP and AG. This suggests that *J. regia* plantation may be more effective in slowing down soil C turnover compared with *R. roxburghii* plantation during ecological restoration. In this study, natural grassland had the highest β value and the lowest $\delta^{13}\text{C}$ fractionation value in the soil profile, suggesting a slower turnover rate of soil C in natural grasslands. Soil aggregate stability is affected by microbial community composition, and a slower SOC turnover rate contributes to the stability of SOC (Chen et al. 2024). Natural grasslands after farmland abandonment have less litter, fewer inputs of fresh SOM, insufficient degradation matrix, and weak decomposition of SOM, root activities, and microorganisms. Therefore, the SOC turnover rate in natural grassland was the lowest compared with all other land uses.

In addition, soil depth also affects the turnover of SOC (Tesfaye et al. 2016). Under the same climatic conditions, the content of SOC is directly related to the characteristics of surface vegetation. This relationship plays a significant role in controlling the distribution of SOC along the soil profile (Jobbágy and Jackson 2000). In this study, the SOC contents decreased with the deepening of the soil layers under different land uses. This can be attributed to the accumulation of dead leaves on the surface soil, which leads to a higher decomposition and turnover rate of SOC due to the increased presence of microorganisms (Chen et al. 2002). As a result, the abundance of surface SOM contributes to the higher content of SOC. From the upper soil to the deeper layers, the sources

of SOM gradually decrease as soil formation time extends. However, the loss caused by SOM decomposition continues to increase (Han et al. 2015). The deeper the soil layer, the fewer the number of microorganisms and the lower the conversion rate of SOM. Therefore, the distribution pattern of SOC content decreased gradually along the soil profile (Chen et al. 2005; Fierer et al. 2003; Zhu and Liu 2006). In the present study, we investigated if soil physicochemical properties could account for the variations in $\delta^{13}\text{C}$ and SOC content. Our results showed that TN content and soil C/N ratio were the main factors explained more than 80% of the variations in $\delta^{13}\text{C}$ and SOC content in this study after running a Monte Carlo test in the RDA (Table 3). The positive coupling relationship between SOC and TN has become a consensus. Mo et al. (2008) reported that the increase of soil nitrogen content will result in a decrease in soil respiration along with a reduction in soil microbial activity, thus leading to a decrease in SOC turnover. Some studies have also indicated that soil C/N ratio is a key factor in relation to the discrimination of stable carbon isotopes in microbial processes such as SOC decomposition and respiration (Powers and Schlesinger 2002; Werth and Kuzyakov 2010). TN is indirectly regulated by changes in plant community composition via its effect on the C/N ratio after farmland abandonment in karst areas, thus affecting the turnover of SOC. Additionally, our study has limitations. Due to the short-term implementation of ecological restoration projects in the study site, our study cannot accurately reflect the impacts of long-term land use changes on the accumulation of SOC. Therefore, this may limit the applicability of the findings of this study.

Conclusions

Economic forest plantations are more effective for SOC accumulation than artificial grass planting and natural revegetation after farmland abandonment in our study area. The input of fresh SOM lead to significant lower $\delta^{13}\text{C}$ values in economic forests and artificial grassland than in natural grassland and farmland at the 0–5 cm depth. And the masking effect of previous soil microorganisms or plant residues may result in insignificant differences in $\delta^{13}\text{C}$ values between farmland and the converted land uses in the subsurface soil layers. We found that the rate of soil

C turnover following afforestation was still higher than that followed by natural revegetation in the short term. Changes in soil $\delta^{13}\text{C}$ and SOC were mainly controlled by TN content and soil C/N ratio. From the perspective of soil carbon sequestration, we suggest that plantation with economic tree species is a beneficial practice for short-term farmland restoration in the karst desertification control. Our results provide an important reference for the protection of soil resources and the adjustment of land use structure in fragile karst ecosystems.

Acknowledgements This research was supported by the Project of Guiyang Engineering Corporation Limited of Power China (Grant No. YJ2023-11), the Key Science and Technology Program of Guizhou Province (No. 5411 2017 QKHP-TRC) and the China Overseas Expertise Introduction Program for Discipline Innovation (D17016).

Declarations

Competing interest The authors declare that there are no conflicts of interest.

References

- Acton P, Fox J, Campbell E, Rowe H, Wilkinson M (2013) Carbon isotopes for estimating soil decomposition and physical mixing in well-drained forest soils. *J Geophys Res: Biogeosci* 118:1532–1545. <https://doi.org/10.1002/2013JG002400>
- Ahmed YA-R, Pichler V, Homolák M, Gömöryová E, Nagy D, Pichlerová M, Gregor J (2012) High organic carbon stock in a karstic soil of the Middle-European Forest Province persists after centuries-long agroforestry management. *Eur J Res* 131:1669–1680. <https://doi.org/10.1007/s10342-012-0608-7>
- Andriollo DD, Redin CG, Reichert JM, da Silva LS (2017) Soil carbon isotope ratios in forest-grassland toposequences to identify vegetation changes in southern Brazilian grasslands. *CATENA* 159:126–135. <https://doi.org/10.1016/j.catena.2017.08.012>
- Battle-Bayer L, Batjes NH, Bindraban PS (2010) Changes in organic carbon stocks upon land use conversion in the Brazilian Cerrado: a review. *Agric Ecosyst Environ* 137:47–58. <https://doi.org/10.1016/j.agee.2010.02.003>
- Bird M, Santrücková H, Lloyd J, Veenendaal E (2001) 1.14 - global soil Organic Carbon Pool. In: E-D Schulze M, Heimann S, Harrison E, Holland J, Lloyd IC, Prentice D, Schimel (eds) *Global biogeochemical cycles in the Climate System*. Academic, San Diego
- Boström B, Comstedt D, Ekblad A (2007) Isotope fractionation and ^{13}C enrichment in soil profiles during

- the decomposition of soil organic matter. *Oecologia* 153:89–98. <https://doi.org/10.1007/s00442-007-0700-8>
- Breecker DO, Bergel S, Nadel M, Tremblay MM, Osuna-Orozco R, Larson TE, Sharp ZD (2015) Minor stable carbon isotope fractionation between respired carbon dioxide and bulk soil organic matter during laboratory incubation of topsoil. *Biogeochemistry* 123:83–98. <https://doi.org/10.1007/s10533-014-0054-3>
- Cai L, Xiong K, Liu Z, Li Y, Fan B (2023) Seasonal variations of plant water use in the karst desertification control. *Sci Total Environ* 885:163778. <https://doi.org/10.1016/j.scitotenv.2023.163778>
- Che L, Cheng M, Xing L, Cui Y, Wan L (2022) Effects of permafrost degradation on soil organic matter turnover and plant growth. *CATENA* 208:105721. <https://doi.org/10.1016/j.catena.2021.105721>
- Chen Q, Shen C, Peng S, Sun Y, Yi W, Li Z, Jiang M (2002) Soil organic matter turnover in the subtropical mountainous region of South China. *Soil Sci* 167:401–415
- Chen Q, Shen C, Sun Y, Peng S, Yi W, Li Z, Jiang M (2005) Spatial and temporal distribution of carbon isotopes in soil organic matter at the Dinghushan Biosphere Reserve, South China. *Plant Soil* 273:115–128. <https://doi.org/10.1007/s11104-004-7245-y>
- Chen X, Zhang X, Zhang Y, Wan C (2009) Carbon sequestration potential of the stands under the Grain for Green Program in Yunnan Province, China. *Ecol Manag* 258:199–206. <https://doi.org/10.1016/j.foreco.2008.07.010>
- Chen Q, Lu S, Xiong K, Zhao R (2021) Coupling analysis on ecological environment fragility and poverty in South China Karst. *Environ Res* 201:111650. <https://doi.org/10.1016/j.envres.2021.111650>
- Chen M, Zhang S, Liu L, Ding X (2023a) Influence of organic fertilization on clay mineral transformation and soil phosphorous retention: evidence from an 8-year fertilization experiment. *Soil Tillage Res* 230:105702. <https://doi.org/10.1016/j.still.2023.105702>
- Chen M, Zhang Y, Gao C, Zhang S, Liu L, Wu L, Li Y, Ding X (2023b) Mineral-microbial interactions in nine-year organic fertilization field experiment: a mechanism for carbon storage in saline-alkaline paddy soil. *Plant Soil* 489:465–481. <https://doi.org/10.1007/s11104-023-06032-4>
- Chen M, Wu L, Ding X, Liu L, Li Y, Fei C, Zhang S (2024) Fe-modified biochar improved the stability of soil aggregates and organic carbon: evidence from enzymatic activity and microbial composition. *Land Degrad Dev* 35:732–743. <https://doi.org/10.1002/ldr.4948>
- Cheng J, Lee X, Theng BKG, Zhang L, Fang B, Li F (2015) Biomass accumulation and carbon sequestration in an age-sequence of *Zanthoxylum bungeanum* plantations under the Grain for Green Program in karst regions, Guizhou Province. *Agric Meteorol* 203:88–95. <https://doi.org/10.1016/j.agrformet.2015.01.004>
- Dai Q, Peng X, Wang P, Li C, Shao H (2018) Surface erosion and underground leakage of yellow soil on slopes in karst regions of southwest China. *Land Degrad Dev* 29:2438–2448. <https://doi.org/10.1002/ldr.2960>
- Deng L, Shangguan Z-p (2017) Afforestation drives soil carbon and nitrogen changes in China. *Land Degrad Dev* 28:151–165. <https://doi.org/10.1002/ldr.2537>
- Di D-R, Huang G-W (2022) Isotope analysis reveals differential impacts of artificial and natural afforestation on soil organic carbon dynamics in abandoned farmland. *Plant Soil* 471:329–342. <https://doi.org/10.1007/s11104-021-05243-x>
- Dong L, Li J, Liu Y, Hai X, Li M, Wu J, Wang X, Shangguan Z, Zhou Z, Deng L (2022) Forestation delivers significantly more effective results in soil C and N sequestrations than natural succession on badly degraded areas: evidence from the Central Loess Plateau case. *CATENA* 208:105734. <https://doi.org/10.1016/j.catena.2021.105734>
- Fierer N, Schimel JP, Holden PA (2003) Variations in microbial community composition through two soil depth profiles. *Soil Biol Biochem* 35:167–176. [https://doi.org/10.1016/S0038-0717\(02\)00251-1](https://doi.org/10.1016/S0038-0717(02)00251-1)
- Ford D, Williams P (2007) Karst hydrogeology. *Karst Hydrogeology and Geomorphology*. <https://doi.org/10.1002/9781118684986.ch5>
- Friedli H, Löttscher H, Oeschger H, Siegenthaler U, Stauffer B (1986) Ice core record of the $^{13}\text{C}/^{12}\text{C}$ ratio of atmospheric CO_2 in the past two centuries. *Nature* 324:237–238. <https://doi.org/10.1038/324237a0>
- Garten CT Jr (2006) Relationships among forest soil C isotopic composition, partitioning, and turnover times. *Can J Res* 36:2157–2167. <https://doi.org/10.1139/x06-115>
- Garten CT Jr, Cooper LW, Post WM III, Hanson PJ (2000) Climate controls on forest soil c isotope ratios in the southern appalachian mountains. *Ecology* 81:1108–1119. [https://doi.org/10.1890/0012-9658\(2000\)081\[1108:CCOFSC\]2.0.CO;2](https://doi.org/10.1890/0012-9658(2000)081[1108:CCOFSC]2.0.CO;2)
- Gautam MK, Lee K-S, Song B-Y, Bong Y-S (2017) Site related $\delta^{13}\text{C}$ of vegetation and soil organic carbon in a cool temperate region. *Plant Soil* 418:293–306. <https://doi.org/10.1007/s11104-017-3284-z>
- Guo Z, Zhang X, Dungait JAJ, Green SM, Wen X, Quine TA (2021) Contribution of soil microbial necromass to SOC stocks during vegetation recovery in a subtropical karst ecosystem. *Sci Total Environ* 761:143945. <https://doi.org/10.1016/j.scitotenv.2020.143945>
- Han G, Li F, Tang Y (2015) Variations in soil organic carbon contents and isotopic compositions under different land uses in a typical karst area in Southwest China. *Geochem J* 49:63–71. <https://doi.org/10.2343/geochemj.2.0331>
- Han G, Tang Y, Liu M, Van Zwieten L, Yang X, Yu C, Wang H, Song Z (2020) Carbon-nitrogen isotope coupling of soil organic matter in a karst region under land use change, Southwest China. *Agric Ecosyst Environ* 301:107027. <https://doi.org/10.1016/j.agee.2020.107027>
- Han C, Song M, Tang Q, Wei J, He X, Collins AL (2023) Post-farming land restoration schemes exhibit higher soil aggregate stability and organic carbon: evidence in the Three Gorges Reservoir Area, China. *CATENA* 227:107099. <https://doi.org/10.1016/j.catena.2023.107099>
- He X, Sheng M, Wang L, Zhang S, Luo N (2022) Effects on soil organic carbon accumulation and mineralization of long-term vegetation restoration in Southwest China karst. *Ecol Indic* 145:109622. <https://doi.org/10.1016/j.ecolind.2022.109622>
- Hobley E, Baldock J, Hua Q, Wilson B (2017) Land-use contrasts reveal instability of subsoil organic carbon. *Global Change Biol* 23:955–965. <https://doi.org/10.1111/gcb.13379>

- Hu C, Fu B, Liu G, Jin T, Guo L (2010) Vegetation patterns influence on soil microbial biomass and functional diversity in a hilly area of the Loess Plateau, China. *J Soils Sediments* 10:1082–1091. <https://doi.org/10.1007/s11368-010-0209-3>
- Hu P, Liu S, Ye Y, Zhang W, He X, Su Y, Wang K (2018) Soil carbon and nitrogen accumulation following agricultural abandonment in a subtropical karst region. *Appl Soil Ecol* 132:169–178. <https://doi.org/10.1016/j.apsoil.2018.09.003>
- Huang Y, Xin Z, Liu J, Liu Q (2022) Divergences of soil carbon turnover and regulation in alpine steppes and meadows on the Tibetan Plateau. *Sci Total Environ* 814:152687. <https://doi.org/10.1016/j.scitotenv.2021.152687>
- Jobbágy EG, Jackson RB (2000) The vertical distribution of soil organic carbon and its relation to climate and vegetation. *Ecol Appl* 10:423–436. [https://doi.org/10.1890/1051-0761\(2000\)010\[0423:TVDOSO\]2.0.CO;2](https://doi.org/10.1890/1051-0761(2000)010[0423:TVDOSO]2.0.CO;2)
- Keiblinger K, Wichern F, Cong W-F (2023) Interplay between living or dead plant carbon input and soil organic matter – key drivers and agricultural management for soil carbon sequestration. *Plant Soil* 488:1–8. <https://doi.org/10.1007/s11104-023-06149-6>
- Kengdo SK, Ahrens B, Tian Y, Heinzle J, Wanek W, Schindlbacher A, Borken W (2023) Increase in carbon input by enhanced fine root turnover in a long-term warmed forest soil. *Sci Total Environ* 855:158800. <https://doi.org/10.1016/j.scitotenv.2022.158800>
- Köchy M, Don A, van der Molen MK, Freibauer A (2015) Global distribution of soil organic carbon – part 2: certainty of changes related to land use and climate. *SOIL* 1:367–380. <https://doi.org/10.5194/soil-1-367-2015>
- Krull ES, Skjemstad JO, Burrows WH, Bray SG, Wynn JG, Bol R, Spouncer L, Harms B (2005) Recent vegetation changes in central Queensland, Australia: evidence from $\delta^{13}\text{C}$ and ^{14}C analyses of soil organic matter. *Geoderma* 126:241–259. <https://doi.org/10.1016/j.geoderma.2004.09.012>
- Lan G, Liu C, Wang H, Tang W, Wu X, Yang H, Tu L, Hu BX, Cao J, Li Q (2021) The effect of land use change and soil redistribution on soil organic carbon dynamics in karst graben basin of China. *J Soils Sediments* 21:2511–2524. <https://doi.org/10.1007/s11368-021-02956-5>
- Li L, Schaeffer SM (2020) Stabilization mechanisms of isotope-labeled carbon substrates in soil under moisture pulses and conservation agricultural management. *Geoderma* 380:114677. <https://doi.org/10.1016/j.geoderma.2020.114677>
- Li D, Niu S, Luo Y (2012) Global patterns of the dynamics of soil carbon and nitrogen stocks following afforestation: a meta-analysis. *New Phytol* 195:172–181. <https://doi.org/10.1111/j.1469-8137.2012.04150.x>
- Li H, Yan F, Tuo D, Yao B, Chen J (2020) The effect of climatic and edaphic factors on soil organic carbon turnover in hummocks based on $\delta^{13}\text{C}$ on the Qinghai-Tibet Plateau. *Sci Total Environ* 741:140141. <https://doi.org/10.1016/j.scitotenv.2020.140141>
- Li B-B, Li P-P, Yang X-M, Xiao H-B, Xu M-X, Liu G-B (2021) Land-use conversion changes deep soil organic carbon stock in the Chinese Loess Plateau. *Land Degrad Dev* 32:505–517. <https://doi.org/10.1002/ldr.3644>
- Li Y, Xiong K, Liu Z, Li K, Luo D (2022) Distribution and influencing factors of soil organic carbon in a typical karst catchment undergoing natural restoration. *CATENA* 212:106078. <https://doi.org/10.1016/j.catena.2022.106078>
- Liu M, Han G, Zhang Q, Song Z (2019) Variations and indications of $\delta^{13}\text{C}_{\text{SOC}}$ and $\delta^{15}\text{N}_{\text{SON}}$ in soil profiles in Karst Critical Zone Observatory (CZO), Southwest China. *Sustainability* 11:2144. <https://doi.org/10.3390/su11072144>
- Liu C, Li Z, Hu BX, Yan J, Xiao H (2020a) Identifying eroded organic matter sources in sediments at fluvial system using multiple tracers on the Loess Plateau of China. *CATENA* 193:104623. <https://doi.org/10.1016/j.catena.2020.104623>
- Liu M, Han G, Zhang Q (2020b) Effects of agricultural abandonment on soil aggregation, soil organic carbon storage and stabilization: results from observation in a small karst catchment, Southwest China. *Agric Ecosyst Environ* 288:106719. <https://doi.org/10.1016/j.agee.2019.106719>
- Lozano-García B, Muñoz-Rojas M, Parras-Alcántara L (2017) Climate and land use changes effects on soil organic carbon stocks in a Mediterranean semi-natural area. *Sci Total Environ* 579:1249–1259. <https://doi.org/10.1016/j.scitotenv.2016.11.111>
- Lozano-García B, Francaviglia R, Renzi G, Doro L, Ledda L, Benítez C, González-Rosado M, Parras-Alcántara L (2020) Land use change effects on soil organic carbon store. An opportunity to soils regeneration in Mediterranean areas: implications in the 4p1000 notion. *Ecol Indic* 119:106831. <https://doi.org/10.1016/j.ecolind.2020.106831>
- Midwood AJ, Boutton TW (1998) Soil carbonate decomposition by acid has little effect on $\delta^{13}\text{C}$ of organic matter. *Soil Biol Biochem* 30:1301–1307. [https://doi.org/10.1016/S0038-0717\(98\)00030-3](https://doi.org/10.1016/S0038-0717(98)00030-3)
- Mo J, Zhang WEI, Zhu W, Gundersen PER, Fang Y, Li D, Wang HUI (2008) Nitrogen addition reduces soil respiration in a mature tropical forest in southern China. *Global Change Biol* 14:403–412. <https://doi.org/10.1111/j.1365-2486.2007.01503.x>
- Paul A, Balesdent J, Hatté C (2020) ^{13}C - ^{14}C relations reveal that soil ^{13}C -depth gradient is linked to historical changes in vegetation ^{13}C . *Plant Soil* 447:305–317. <https://doi.org/10.1007/s11104-019-04384-4>
- Powers JS, Schlesinger WH (2002) Geographic and vertical patterns of stable carbon isotopes in tropical rain forest soils of Costa Rica. *Geoderma* 109:141–160. [https://doi.org/10.1016/S0016-7061\(02\)00148-9](https://doi.org/10.1016/S0016-7061(02)00148-9)
- Qiao Y, Miao S, Li N, Xu Y, Han X, Zhang B (2015) Crop species affect soil organic carbon turnover in soil profile and among aggregate sizes in a Mollisol as estimated from natural ^{13}C abundance. *Plant Soil* 392:163–174. <https://doi.org/10.1007/s11104-015-2414-8>
- Qu Q, Zhang J, Hai X, Wu J, Fan J, Wang D, Li J, Shangguan Z, Deng L (2022) Long-term fencing alters the vertical distribution of soil $\delta^{13}\text{C}$ and SOC turnover rate: revealed by MBC- $\delta^{13}\text{C}$. *Agric Ecosyst Environ* 339:108119. <https://doi.org/10.1016/j.agee.2022.108119>
- Sanderman J, Hengl T, Fiske GJ (2017) Soil carbon debt of 12,000 years of human land use. *P Natl Acad Sci* 114:9575–9580. <https://doi.org/10.1073/pnas.1706103114>
- Schellekens J, Justi M, Macedo R, Calegari MR, Buurman P, Kuyper TW, Barbosa de Camargo P, Vidal-Torrado P

- (2023) Long-term carbon storage in Brazilian Cerrado soils – a conjunction of wildfires, bioturbation, and local edaphic controls on vegetation. *Plant Soil* 484:645–662. <https://doi.org/10.1007/s11104-022-05824-4>
- Tesfaye MA, Bravo F, Ruiz-Peinado R, Pando V, Bravo-Oviedo A (2016) Impact of changes in land use, species and elevation on soil organic carbon and total nitrogen in Ethiopian Central Highlands. *Geoderma* 261:70–79. <https://doi.org/10.1016/j.geoderma.2015.06.022>
- Tong X, Brandt M, Yue Y, Horion S, Wang K, Keersmaecker WD, Tian F, Schurgers G, Xiao X, Luo Y, Chen C, Myneni R, Shi Z, Chen H, Fensholt R (2018) Increased vegetation growth and carbon stock in China karst via ecological engineering. *Nat Sustain* 1:44–50. <https://doi.org/10.1038/s41893-017-0004-x>
- Torn MS, Lapenis AG, Timofeev A, Fischer ML, Babikov BV, Harden JW (2002) Organic carbon and carbon isotopes in modern and 100-year-old-soil archives of the Russian steppe. *Global Change Biol* 8:941–953. <https://doi.org/10.1046/j.1365-2486.2002.00477.x>
- Veloso MG, Dieckow J, Zanatta JA, Bayer C, Higa RCV, Brevilieri RC, Comerford NB, Stoppe AM (2018) Reforestation with loblolly pine can restore the initial soil carbon stock relative to a subtropical natural forest after 30 years. *Eur J Res* 137:593–604. <https://doi.org/10.1007/s10342-018-1127-y>
- Wang C, Wei H, Liu D, Luo W, Hou J, Cheng W, Han X, Bai E (2017) Depth profiles of soil carbon isotopes along a semi-arid grassland transect in northern China. *Plant Soil* 417:43–52. <https://doi.org/10.1007/s11104-017-3233-x>
- Wang C, Houlton BZ, Liu D, Hou J, Cheng W, Bai E (2018) Stable isotopic constraints on global soil organic carbon turnover. *Biogeosciences* 15:987–995. <https://doi.org/10.5194/bg-15-987-2018>
- Wang X, Huang X, Xiong K, Hu J, Zhang Z, Zhang J (2022a) Mechanism and evolution of Soil Organic Carbon Coupling with Rocky Desertification in South China Karst. *Forests* 13:28. <https://doi.org/10.3390/f13010028>
- Wang X, Liu Z, Xiong K, He Q, Li Y, Li K (2022b) Characteristics and controlling factors of soil dissolved organic matter in the rainy season after vegetation restoration in a karst drainage area, South China. *CATENA* 217:106483. <https://doi.org/10.1016/j.catena.2022.106483>
- Wedin DA, Tieszen LL, Dewey B, Pastor J (1995) Carbon Isotope dynamics during grass decomposition and soil organic matter formation. *Ecology* 76:1383–1392. <https://doi.org/10.2307/1938142>
- Werth M, Kuzyakov Y (2010) ^{13}C fractionation at the root-microorganisms–soil interface: a review and outlook for partitioning studies. *Soil Biol Biochem* 42:1372–1384. <https://doi.org/10.1016/j.soilbio.2010.04.009>
- Wynn JG, Bird MI, Wong VNL (2005) Rayleigh distillation and the depth profile of $^{13}\text{C}/^{12}\text{C}$ ratios of soil organic carbon from soils of disparate texture in Iron Range National Park, Far North Queensland, Australia. *Geochim Cosmochim Acta* 69:1961–1973. <https://doi.org/10.1016/j.gca.2004.09.003>
- Wynn JG, Harden JW, Fries TL (2006) Stable carbon isotope depth profiles and soil organic carbon dynamics in the lower Mississippi Basin. *Geoderma* 131:89–109. <https://doi.org/10.1016/j.geoderma.2005.03.005>
- Xiao J, Xiong K (2022) A review of agroforestry ecosystem services and its enlightenment on the ecosystem improvement of rocky desertification control. *Sci Total Environ* 852:158538. <https://doi.org/10.1016/j.scitotenv.2022.158538>
- Xiao K, He T, Chen H, Peng W, Song T, Wang K, Li D (2017) Impacts of vegetation restoration strategies on soil organic carbon and nitrogen dynamics in a karst area, southwest China. *Ecol Eng* 101:247–254. <https://doi.org/10.1016/j.ecoleng.2017.01.037>
- You M, Han X, Chen X, Yan J, Li N, Zou W, Lu X, Li Y, Horwath WR (2019) Effect of reduction of aggregate size on the priming effect in a Mollisol under different soil managements. *Eur J Soil Sci* 70:765–775. <https://doi.org/10.1111/ejss.12818>
- You M, Zhu-Barker X, Hao X-X, Li L-J (2021) Profile distribution of soil organic carbon and its isotopic value following long term land-use changes. *CATENA* 207:105623. <https://doi.org/10.1016/j.catena.2021.105623>
- Zeng C, Liu Z, Zhao M, Yang R (2016) Hydrologically-driven variations in the karst-related carbon sink fluxes: insights from high-resolution monitoring of three karst catchments in Southwest China. *J Hydrol* 533:74–90. <https://doi.org/10.1016/j.jhydrol.2015.11.049>
- Zhang H, Wang K, Zeng Z, Du H, Zeng F (2017) Biomass and carbon sequestration by Juglans regia plantations in the Karst regions of Southwest China. *Forests* 8:103. <https://doi.org/10.3390/f8040103>
- Zhang Z, Huang X, Zhou Y (2020) Spatial heterogeneity of soil organic carbon in a karst region under different land use patterns. *Ecosphere* 11:e03077. <https://doi.org/10.1002/ecs2.3077>
- Zhao Y, Wang X, Ou Y, Jia H, Li J, Shi C, Liu Y (2019) Variations in soil $\delta^{13}\text{C}$ with alpine meadow degradation on the eastern Qinghai–Tibet Plateau. *Geoderma* 338:178–186. <https://doi.org/10.1016/j.geoderma.2018.12.005>
- Zhao F, Wu Y, Yin X, Alexandrov G, Qiu L (2022) Toward sustainable revegetation in the Loess Plateau using coupled Water and Carbon Management. *Engineering* 15:143–153. <https://doi.org/10.1016/j.eng.2020.12.017>
- Zhao Z, Dong P, Fu B, Wu D, Zhao Z (2023) Soil organic carbon distribution and factors affecting carbon accumulation in natural and plantation forests in tropical China. *Ecol Indic* 148:110127. <https://doi.org/10.1016/j.ecolind.2023.110127>
- Zhu S, Liu C (2006) Vertical patterns of stable carbon isotope in soils and particle-size fractions of karst areas, Southwest China. *Environ Geol* 50:1119–1127. <https://doi.org/10.1007/s00254-006-0285-2>

Publisher's Note Springer Nature remains neutral with regard to jurisdictional claims in published maps and institutional affiliations.

Springer Nature or its licensor (e.g. a society or other partner) holds exclusive rights to this article under a publishing agreement with the author(s) or other rightsholder(s); author self-archiving of the accepted manuscript version of this article is solely governed by the terms of such publishing agreement and applicable law.